

$D_s^+ \rightarrow \pi^+\pi^+\pi^-$ decay: the $1^3P_0 s\bar{s}$ component in scalar-isoscalar mesons

V.V. Anisovich, L.G. Dakhno and V.A. Nikonov

February 17, 2003

Abstract

On the basis of data on the decay $D_s^+ \rightarrow \pi^+\pi^+\pi^-$, which goes dominantly via the transition $D_s \rightarrow \pi^+ s\bar{s}$, we evaluate the $1^3P_0 s\bar{s}$ components in the scalar-isoscalar resonances $f_0(980)$, $f_0(1300)$, $f_0(1500)$ and broad state $f_0(1200 - 1600)$. The data point to a large $s\bar{s}$ component in the $f_0(980)$: $40\% \lesssim s\bar{s} \lesssim 70\%$. Nearly 30% of the $1^3P_0 s\bar{s}$ component flows to the mass region 1300–1500 MeV being shared by $f_0(1300)$, $f_0(1500)$ and broad state $f_0(1200 - 1600)$: the interference of these states results in a peak near 1400 MeV with the width around 200 MeV.

1 Introduction

The meson yields in the decay $D_s^+ \rightarrow \pi^+\pi^+\pi^-$ [1] evoked immediately a great interest and now they are actively discussed (see [2, 3, 4, 5] and references therein). The matter is that in this decay the production of strange quarkonium is dominant, $D_s^+ \rightarrow \pi^+ s\bar{s}$, with a subsequent transition $s\bar{s} \rightarrow f_J \rightarrow \pi^+\pi^-$. Therefore, the reaction $D_s^+ \rightarrow \pi^+\pi^+\pi^-$ may serve us as a tool for the estimation of $s\bar{s}$ components in the f_J mesons. This possibility is particularly important in context of the determination of quark content of the f_0 mesons, for the classification of $q\bar{q}$ scalar-isoscalar states is a key problem in the search for exotics.

In the D_s^+ decay the production of f_0 mesons proceeds mainly via spectator mechanism, Fig. 1a: this very mechanism implements the transition $s\bar{s} \rightarrow f_0$. Besides, the spectator mechanism provides a strong production of the $\phi(1020)$ meson. To evaluate the $s\bar{s}$ components in f_0 mesons, we use the process $D_s^+ \rightarrow \pi^+\phi(1020)$ as a standard: we consider the ratio $D_s^+ \rightarrow \pi^+ f_0 / D_s^+ \rightarrow \pi^+ \phi(1020)$, where the uncertainty related to the coupling $c \rightarrow \pi^+ s$ is absent.

Calculation of the transition of Fig. 1a is performed in the spectral integration technique, this technique was intensively used for the study of weak decays of D

and B mesons, see [6] and references therein. The cuttings of the triangle diagram related to the double spectral integrals are shown in Fig. 1b.

In addition, the $\pi^+ f_0$ production can originate from the W -annihilation process of Figs. 1c,d. It is a relatively weak transition, nevertheless we take it into account, and the reaction $D_s^+ \rightarrow \pi^+ \rho^0$ serves us as a scale to determine the W -annihilation coupling $c\bar{s} \rightarrow u\bar{d}$. Let us emphasize that the processes shown in Fig. 1 are of the leading order in terms of the $1/N_c$ expansion rule.

In Section 2 we present the data set used for the analysis and write down the amplitudes for the spectator and W -annihilation processes. The results of calculations are presented and discussed in Section 3. In this Section we demonstrate that (i) the W -annihilation contributes weakly to the f_J -meson production, and (ii) the 1^3P_0 -state dominates the transition $s\bar{s} \rightarrow f_0$, while the production of the $2^3P_0 s\bar{s}$ -component is relatively suppressed, so the transition $D_s^+ \rightarrow \pi^+ s\bar{s} \rightarrow \pi^+ f_0$ is in fact a measure for the $1^3P_0 s\bar{s}$ -component in scalar-isoscalar mesons.

In Conclusion we sum up what the data on the decay $D_s^+ \rightarrow \pi^+ \pi^+ \pi^-$ tell us, in particular with respect to the identification of the lightest scalar $q\bar{q}$ nonet.

2 Data set and the amplitudes for the spectator and W -annihilation mechanisms

In this Section we present the data used in the analysis and write formulae for the spectator and W -annihilation mechanisms, Fig. 1a and Figs. 1c,d, respectively.

2.1 The data set

In the recently measured spectra from the reaction $D_s^+ \rightarrow \pi^+ \pi^+ \pi^-$ [1], the relative weight of channels $\pi^+ f_0(980)$ and $\pi^+ \rho^0(770)$ is evaluated,

$$BR(\pi^+ f_0(980)) = 57\% \pm 9\%, \quad BR(\pi^+ \rho^0(770)) = 6\% \pm 6\%, \quad (1)$$

and the ratio of yields,

$$\Gamma(D_s^+ \rightarrow \pi^+ \pi^+ \pi^-) / \Gamma(D_s^+ \rightarrow \pi^+ \phi(1020)) = 0.245 \pm 0.028^{+0.019}_{-0.012} \quad (2)$$

is measured. These values are the basis to determine relative weight of the $s\bar{s}$ component in the $f_0(980)$.

Besides, in ref. [1] the bump in the wave ($IJ^{PC} = 00^{++}$) is seen at 1434 ± 18 MeV with the width 173 ± 32 MeV; this should be a contribution from the nearly located resonances $f_0(1300)$, $f_0(1500)$ and the broad state $f_0(1200 - 1600)$. Relative weight of this bump is equal to:

$$BR(\pi^+(f_0(1300) + f_0(1500) + f_0(1200 - 1600))) = 26\% \pm 11\%. \quad (3)$$

This magnitude allows us to determine the total weight of the $1^3P_0 s\bar{s}$ component in the states $f_0(1300)$, $f_0(1500)$, $f_0(1200 - 1600)$.

Now the data of FOCUS collaboration [7] on the decay $D_s \rightarrow \pi^+ f_0(980)$ are available. These data are compatible with those of [1], so we do not use them in our estimates, and we base on the ratios $\pi^+ f_0 / \pi^+ \phi$ measured in [1].

In addition, the production of $f_2(1270)$ is seen in [1]: $BR(\pi^+ f_2(1270)) = 20\% \pm 4\%$ that makes it necessary to include tensor mesons into the calculation machinery.

2.2 Decay amplitudes and partial widths

The spin structure of the amplitude depends on the type of the produced meson — it is different for scalar (f_0), vector (ϕ, ω, ρ) or tensor (f_2) mesons. Let us denote the momenta of the produced scalar (S), vector (V) and tensor (T) mesons by p_M where $M = S, V, T$; the D_s -meson momentum is referred as p .

The production amplitude is written as

$$A(D_s \rightarrow \pi^+ M) = \hat{O}_M(p, p_M) A_M(q^2), \quad (4)$$

where the spin operators $\hat{O}_M(p, p_M)$ for scalar, vector and tensor mesons read as follows:

$$\hat{O}_S(p, p_S) = 1, \quad \hat{O}_V(p, p_V) = p_{V\perp\mu}, \quad \hat{O}_T(p, p_T) = \frac{p_{T\perp\mu} p_{T\perp\nu}}{p_{T\perp}^2} - \frac{1}{3} g_{\mu\nu}^\perp. \quad (5)$$

The momenta $p_{V\perp}$ and $p_{T\perp}$ are orthogonal to the D_s -meson momentum p :

$$p_{V\perp\mu} = g_{\mu\mu'}^\perp p_{V\mu'}, \quad p_{T\perp\mu} = g_{\mu\mu'}^\perp p_{T\mu'}, \quad g_{\mu\mu'}^\perp = g_{\mu\mu'} - \frac{p_\mu p_{\mu'}}{p^2}. \quad (6)$$

In the spectral integration technique, the invariant production amplitude $A_M(q^2)$ is calculated as a function of $q^2 = (p - p_M)^2 = m_\pi^2$.

In terms of the spin-dependent operators $\hat{O}_M(p, p_M)$, partial width for the transition $D_s^+ \rightarrow \pi^+ M$ reads:

$$m_{D_s} \Gamma(D_s^+ \rightarrow \pi^+ M) = \left| F_M(q^2 = m_\pi^2) \right|^2 \left(\hat{O}_M(p, p_M) \right)^2 \frac{\sqrt{-p_{M\perp}^2}}{8\pi m_{D_s}}, \quad (7)$$

where

$$\left(\hat{O}_S(p, p_S) \right)^2 = 1, \quad \left(\hat{O}_V(p, p_V) \right)^2 = -p_{V\perp\mu}^2, \quad \left(\hat{O}_T(p, p_T) \right)^2 = \frac{2}{3}. \quad (8)$$

In (7), the value $\sqrt{-p_{M\perp}^2}$ is equal to the center-of-mass relative momentum of mesons in the final state; it is determined by the magnitudes of the meson masses as follows:

$$\sqrt{-p_{M\perp}^2} = \sqrt{[m_{D_s}^2 - (m_M + m_\pi)^2][m_{D_s}^2 - (m_M - m_\pi)^2]} / 2m_{D_s}.$$

2.3 Amplitudes for the spectator and W -annihilation processes in the light-cone variables

In the leading order of the $1/N_c$ expansion, there exist two types of processes which govern the decays $D_s^+ \rightarrow \pi^+ f_0, \pi^+ f_2, \pi^+ \phi/\omega, \pi^+ \rho^0$. They are shown in Figs. 1a,c,d. We refer to the process of Fig. 1a as a spectator one, while that shown in Fig. 1c,d is called the W -annihilation process. The transition $s\bar{s} \rightarrow \text{meson}$ is a characteristic feature of the spectator mechanism, it contributes to the production of isoscalar mesons: $D_s^+ \rightarrow \pi^+ f_0, \pi^+ f_2, \pi^+ \phi, \pi^+ \omega$, whereas ρ^0 cannot be produced within spectator mechanism. The W -annihilation contributes to the production of mesons with both $I = 1$ and $I = 0$, $D_s^+ \rightarrow \pi^+ f_0, \pi^+ f_2, \pi^+ \phi, \pi^+ \omega$ and $D_s \rightarrow \pi^+ \rho^0$. Therefore, the latter reaction, $D_s \rightarrow \pi^+ \rho^0$, allows us to evaluate relative weight of the effective coupling constant for W -annihilation, thus giving a possibility to estimate the W -annihilation contribution to the channels of interest: $D_s^+ \rightarrow \pi^+ f_0, \pi^+ f_2, \pi^+ \phi$. This estimate tells us that the W -annihilation is relatively weak that agrees with conventional evaluations, see, for example, [6].

The amplitudes for the spectator production of mesons (Fig. 1a) and for W -annihilation (Figs. 1c,d) can be calculated in terms of double spectral integral representation developed for the quark three-point diagrams in [6, 8]. The calculation scheme for the diagram of Fig. 1a in the spectral integration technique is as follows. We consider the relevant energy-off-shell diagram shown in Fig. 1b for which the momentum of the $c\bar{s}$ system, $P = k_1 + k_2$, obeys the requirement $P^2 \equiv s > (m_c + m_s)^2$, while the $s\bar{s}$ system, with the momentum $P' = k'_1 + k_2$, satisfies the constraint $P'^2 \equiv s' > 4m_s^2$, here $m_{s,c}$ are the masses of the constituent s, c quarks which are taken to be $m_s = 500$ MeV and $m_c = 1500$ MeV. The next step consists in the calculation of double discontinuity of the triangle diagram (cuttings I and II in Fig. 1b) which correspond to real processes, and the double discontinuity is the integrand of double dispersion representation.

The double dispersion integrals may be rewritten in terms of the light-cone variables, by introducing the light-cone wave functions for the D_s^+ -meson and produced mesons $f_0, f_2, \phi, \omega, \rho^0$: the calculations performed here are done by using these variables.

Our calculations have been carried out in the limit of negligibly small pion mass, $m_\pi \rightarrow 0$, that is a reasonable approach, for in the ratio $D_s \rightarrow \pi^+ f_J / D_s \rightarrow \pi^+ \phi$ the uncertainties related to this limit are mainly cancelled.

2.3.1 Spectator-production form factor

The form factor for the spectator process given by the triangle diagram of Fig. 1a reads:

$$F_M^{(spectator)}(q^2) = \frac{G_{spectator}}{16\pi^3} \int_0^1 \frac{dx}{x(1-x)^2} \int d^2k_\perp \psi_{D_s}(s) \psi_M(s') S_{D_s \rightarrow \pi M}(s, s', q^2) . \quad (9)$$

Here $G_{spectator}$ is the vertex for the decay transition $c \rightarrow \pi^+ s$; the light-cone variables x and \mathbf{k}_\perp refer to the momenta of quarks in the intermediate states. The energies squared for initial and final quark states ($c\bar{s}$ and $s\bar{s}$) are written in terms of the light-cone variables as follows:

$$s = \frac{m_c^2 + k_\perp^2}{1-x} + \frac{m_s^2 + k_\perp^2}{x} , \quad s' = \frac{m_s^2 + (\mathbf{k}_\perp + x\mathbf{q}_\perp)^2}{x(1-x)} . \quad (10)$$

The limit of the negligibly small pion mass corresponds to $\mathbf{q}_\perp \rightarrow 0$; in (9) this limit is attained within numerical calculation of $F_M^{(spectator)}(q^2)$ at small negative q^2 .

In the spectral integration technique, wave functions of the initial and final states are determined as ratios of vertices to the dispersion-relation denominators, $\psi_{D_s \rightarrow c\bar{s}}(s) = G_{D_s \rightarrow c\bar{s}}(s)/(s - m_{D_s}^2)$ and $\psi_{M \rightarrow s\bar{s}}(s') = G_{M \rightarrow s\bar{s}}(s')/(s' - m_M^2)$, see [6, 8] for details.

In our calculations, the D_s^+ -meson wave functions and $s\bar{s}$ component are parametrized as follows:

$$\psi_{D_s=c\bar{s}}(s) = C_D \exp(-b_D s) , \quad \psi_M(s') = C_M \exp(-b_M s') , \quad (11)$$

where C_D and C_M are the normalization constants for the wave functions and b_D and b_M characterize the mean radii squared of the $c\bar{s}$ and $s\bar{s}$ systems, $R_{D_s}^2$ and R_M^2 . In the approximation (11), the mean radii squared are the only parameters for the description of quark wave functions. Based on the results of the analysis of the radiative decays [9] we put R_M^2 for $f_0(980)$, $\phi(1020)$ and $f_2(1270)$ to be of the order of the pion radius squared, $R_M^2 \sim R_\pi^2 = 10 \text{ GeV}^{-2}$, that corresponds to the following wave function parameters for $s\bar{s}$ components (in GeV units):

$$b_{f_0(980)} = 1.25, \quad b_{\phi(1020)} = 2.50, \quad b_{f_2(1270)} = 1.25, \quad (12)$$

$$C_{f_0(980)} = 98.92, \quad C_{\phi(1020)} = 374.76, \quad C_{f_2(1270)} = 68.85 .$$

Recall that in [9] the mean radius squared was defined through the Q^2 -dependence of meson form factor at small momentum transfers, $F_M(Q^2) \simeq 1 - Q^2 R_M^2/6$, and the normalization factor C_M is given by $F_M(0) = 1$, that actually represents the convolution $\psi_M \otimes \psi_M = 1$.

For the D_s^+ -meson, the charge radius squared $R_{D_s}^2$ is of the order of $3.5 \div 5.5 \text{ GeV}^{-2}$ [6] that corresponds to

$$b_{D_s} \simeq (0.70 \div 1.50) \text{ GeV}^{-2} , \quad C_{D_s} \simeq (157.6 \div 7205.4) \text{ GeV}^{-2} . \quad (13)$$

One should keep in mind that the D_s^+ -meson charge radius squared is determined by two form factors, $F_c(Q^2)$ and $F_{\bar{s}}(Q^2)$, when the photon interacts with c and \bar{s} quarks: $2F_c(Q^2)/3 + F_{\bar{s}}(Q^2)/3 \simeq 1 - R_{D_s}^2 Q^2/6$.

The factor $S_{D_s \rightarrow \pi M}(s, s', q^2)$ is defined by the spin structure of the quark loop in the diagram of Fig. 1b. Corresponding trace of the three-point quark loop is equal to:

$$\hat{S}_M = -\text{Tr} \left[\hat{Q}_M(-\hat{k}_2 + m_s) i\gamma_5(\hat{k}_1 + m_c) i\gamma_5(\hat{k}'_1 + m_s) \right], \quad (14)$$

where $i\gamma_5$ stands for the D_s -meson and pion vertices, and \hat{Q}_M is the spin operator for the transition ($s\bar{s} \rightarrow \text{meson } M$) which is defined for scalar, vector and tensor mesons as follows:

$$\begin{aligned} \hat{Q}_S &= 1, \\ \hat{Q}_V &= \gamma'_{\perp\mu}, \\ \frac{1}{2}\hat{Q}_T &= k'_\mu \gamma'_{\perp\nu} + k'_\nu \gamma'_{\perp\mu} - \frac{2}{3} \hat{k}' g'^\perp_{\mu\nu}. \end{aligned} \quad (15)$$

Here $k' = (k'_1 - k_2)/2$ and $\gamma'_{\perp\mu} = g'^\perp_{\mu\nu} \gamma_{\perp\nu}$, where $g'^\perp_{\mu\nu} = g_{\mu\nu} - P'_\mu P'_\nu / P'^2$. The operator \hat{Q}_T stands for the production of f_2 -mesons belonging to the basic $1^3P_2 q\bar{q}$ multiplet.

With these definitions, the factor $\hat{S}_{D_s \rightarrow \pi M}(s, s', q^2)$ can be calculated through normalized convolution of the quark-loop operator (14) with the spin operator of the amplitude given by (5) but determined in the space of internal momenta, by substituting $p \rightarrow P$ and $p_M \rightarrow P'$, namely,

$$S_{D_s \rightarrow \pi M}(s, s', q^2) = \frac{(\hat{S}_M \cdot \hat{O}_M(P, P'))}{(\hat{O}_M(P, P'))^2}. \quad (16)$$

Let us emphasize once again, that we calculate the integrand of the spectral integral for the energy-off-shell process of Fig. 1b. Because of that, the invariant spin-dependent structure $S_{D_s \rightarrow \pi M}(s, s', q^2)$ should be calculated through (16) with the energy-off-shell operators $\hat{O}_M(P, P')$ and mass-on-shell constituents. The spin factors determined by (16) read:

$$\begin{aligned} S_{D_s \rightarrow \pi f_0}(s, s', q^2) &= 2(sm_s - 2m_c^2 m_s - m_c s' + 4m_c m_s^2 + q^2 m_s - 2m_s^3), \\ S_{D_s \rightarrow \pi \phi/\omega}(s, s', q^2) &= \frac{-8s'}{\lambda} (sm_c^2 - sm_c m_s - sq^2 - m_c^4 + 2m_c^3 m_s - m_c^2 s' \\ &\quad + m_c^2 q^2 + m_c s' m_s - m_c q^2 m_s - 2m_c m_s^3 + m_s^4), \\ S_{D_s \rightarrow \pi f_2}(s, s', q^2) &= \frac{8s'}{\lambda} (sm_c^2 - sm_c m_s - sq^2 - m_c^4 + 2m_c^3 m_s - m_c^2 s' \\ &\quad + m_c^2 q^2 + m_c s' m_s - m_c q^2 m_s - 2m_c m_s^3 + m_s^4) \\ &\quad \times (s - 2m_c^2 - s' + q^2 + 2m_s^2), \end{aligned} \quad (17)$$

where $\lambda = (s' - s)^2 - 2q^2(s' + s) + q^4$. In the performed calculations we have used the moment-expansion technique, for the details see the review paper [10] and references therein.

2.3.2 W -annihilation form factor

The right-hand side three-point block of Fig. 1c,d which describes the transitions of the $u\bar{d}$ system into mesons $\pi^+ M$ can be also calculated with the formulae similar to (9). One has:

$$F_M^{(W)}(q^2) = \frac{1}{16\pi^3} \int_0^1 \frac{dx}{x(1-x)^2} \int d^2 k_\perp \frac{G_w}{s - m_{D_s}^2 - i0} \psi_M(s') S_{D_s(u\bar{d}) \rightarrow \pi M}(s, s', q^2) . \quad (18)$$

For the transition $D_s^+ \rightarrow u\bar{d}$ we use the dispersion relation description, and vertex G_W is treated as energy-independent factor.

The spin factor $S_{D_s(u\bar{d}) \rightarrow \pi M}(s, s', q^2)$ is determined by the triangle graph of Fig. 1c,d, with light quarks in the intermediate state. Therefore,

$$\hat{S}_M^{(W)} = -\text{Tr} \left[\hat{Q}_M(-\hat{k}_2 + m) i\gamma_5 (\hat{k}_1 + m) i\gamma_5 (\hat{k}'_1 + m) \right] , \quad (19)$$

where $m = 350$ MeV, and \hat{Q}_M is given by (15). Furthermore, the spin factors $S_{D_s(u\bar{d}) \rightarrow \pi M}(s, s', q^2)$ is calculated with the use of (16). For scalar, vector and tensor mesons, respectively, they are equal to

$$\begin{aligned} S_{D_s(u\bar{d}) \rightarrow \pi f_0}(s, s', q^2) &= 2m(s - s' + q^2) , \\ S_{D_s(u\bar{d}) \rightarrow \pi \phi / \omega}(s, s', q^2) &= \frac{8ss'q^2}{\lambda} , \\ S_{D_s(u\bar{d}) \rightarrow \pi f_2}(s, s', q^2) &= -\frac{8ss'q^2}{\lambda}(s - s' + q^2) . \end{aligned} \quad (20)$$

The transition amplitude defined by Eq. (18) is complex-valued.

3 Calculations and results

Here we write down the amplitudes used for the calculation of the decay processes — corresponding results are presented below.

3.1 Amplitudes for decay channels $\pi^+ f_0(980)$, $\pi^+ \phi(1020)$, $\pi^+ f_2(1270)$, $\pi^+ \rho^0$

Taking into account two decay processes, spectator and W -annihilation, we write the transition amplitude as follows:

$$A(D_s \rightarrow \pi^+ M) = \xi_M^{(spectator)} F_M^{(spectator)}(0) + \xi_M^{(W)} F_M^{(W)}(0) , \quad (21)$$

where the factors $\xi^{(spectator)}$ and $\xi^{(W)}$ are determined by flavour content of isoscalar mesons. In terms of the quarkonium states $s\bar{s}$ and $n\bar{n} = (u\bar{u} + d\bar{d})/\sqrt{2}$, we define flavour wave functions of isoscalar mesons as

$$\begin{aligned}\phi(1020) &: n\bar{n} \sin \varphi_V + s\bar{s} \cos \varphi_V, \\ f_0(980) &: n\bar{n} \cos \varphi[f_0(980)] + s\bar{s} \sin \varphi[f_0(980)], \\ f_2(1270) &: n\bar{n} \cos \varphi_T + s\bar{s} \sin \varphi_T.\end{aligned}\tag{22}$$

that serves us for the determination of coefficients in (21):

$$\begin{aligned}D_s^+ \rightarrow \pi^+ \phi(1020) &: \xi_\phi^{spectator} = \cos \varphi_V, \quad \xi_\phi^W = \sqrt{2} \sin \varphi_V, \\ D_s^+ \rightarrow \pi^+ f_0(980) &: \xi_{f_0(980)}^{spectator} = \sin \varphi[f_0(980)], \quad \xi_{f_0(980)}^W = \sqrt{2} \cos \varphi[f_0(980)], \\ D_s^+ \rightarrow \pi^+ f_2(1270) &: \xi_{f_2(1270)}^{spectator} = \sin \varphi_T, \quad \xi_{f_2(1270)}^W = \sqrt{2} \cos \varphi_T.\end{aligned}\tag{23}$$

For $\phi(1020)$, which is dominantly the $s\bar{s}$ state, we fix mixing angle in the interval $|\varphi_V| \leq 4^\circ$.

The production of $\pi^+ \rho^0$ is due to the direct mechanism only:

$$D_s^+ \rightarrow \pi^+ \rho^0 : \quad \xi_\rho^{(spectator)} = 0, \quad \xi_\rho^{(W)} = \sqrt{2}.\tag{24}$$

3.2 Evaluation of the ratio $G_W/G_{spectator}$

To evaluate the ratio $G_W/G_{spectator}$ we use the reaction $D_s^+ \rightarrow \pi^+ \rho^0$, with the experimental constraint $\Gamma(\pi^+ \rho^0)/\Gamma(\pi^+ \phi) \leq 0.032$. By using maximal value of $\Gamma(\pi^+ \rho^0)/\Gamma(\pi^+ \phi) = 0.032$ we get the following ratios $F_M^{(W)}(0)/F_M^{(spectator)}(0)$ for scalar, vector and tensor mesons at $R_{D_s}^2 = 4.5 \text{ GeV}^{-2}$:

$$\begin{aligned}\frac{\sqrt{2}F_S^{(W)}(0)}{F_S^{(spectator)}} &= (0.28 + i0.75) \cdot 10^{-3}, \\ \frac{\sqrt{2}F_V^{(W)}(0)}{F_V^{(spectator)}} &= (0.5 + i15.1) \cdot 10^{-2}, \\ \frac{\sqrt{2}F_T^{(W)}(0)}{F_T^{(spectator)}} &= (0.26 + i1.35) \cdot 10^{-3}.\end{aligned}\tag{25}$$

This evaluation tells us that the W -annihilation contribution is comparatively small, and one may neglect it when the reactions $D_s^+ \rightarrow \pi^+ f_0$ and $D_s^+ \rightarrow \pi^+ f_2$ are studied.

3.3 Evaluation of relative weights of the $1^3P_0 s\bar{s}$ and $2^3P_0 s\bar{s}$ states for the decay $D_s^+ \rightarrow \pi^+ f_0$

In the region 1000–1500 MeV one can expect the existence of scalar-isoscalar states which belong to the basic and first radial-excitation $q\bar{q}$ -nonets, 1^3P_0 and 2^3P_0 . Here

we estimate relative weights of the states $1^3P_0s\bar{s}$ and $2^3P_0s\bar{s}$ in the transitions $D_s^+ \rightarrow \pi^+ s\bar{s} \rightarrow \pi^+ f_0$.

The form factor for the production of radial-excitation state is given by (9), with a choice of the wave function as follows:

$$\psi_{M(rad. excit.)}(s') = C_{rad. excit.}(d_{rad. excit.}s' - 1) \exp(-b_{rad. excit.}s') , \quad (26)$$

Two parameters in (26) can be determined by the normalization and orthogonality conditions, $\psi_{M(rad. excit.)} \otimes \psi_{M(rad. excit.)} = 1$ and $\psi_{M(rad. excit.)} \otimes \psi_{M(basic)} = 0$, while the third one can be related to the mean radius squared, $R_{rad. excit.}^2$. In our estimates we keep $R_{rad. excit.}^2$ to be of the order of pion radius squared, or larger, $1 \leq R_{rad. excit.}^2/R_\pi^2 \leq 1.5$. To be precise, we present as an example the wave function parameters (in GeV units) for $2^3P_0s\bar{s}$ state with $R_{rad. excit.}^2 = 11.3 \text{ GeV}^{-2}$:

$$b_{rad. excit.} = 1.75, \quad C_{rad. excit.} = 938.5, \quad d_{rad. excit.} = 0.60. \quad (27)$$

In Fig. 2 we show the ratios

$$\frac{\Gamma(D_s^+ \rightarrow \pi^+(2^3P_0s\bar{s}))}{\Gamma(D_s^+ \rightarrow \pi^+(1^3P_0s\bar{s}))}$$

for different values of radius square of the $(2^3P_0s\bar{s})$ component, $R^2(f_0^{rad. excit.})$, in the interval $3.5 \lesssim R_{D_s}^2 \lesssim 5.5 \text{ GeV}^{-2}$.

From the point of view of the calculation technique, a suppression of the production of the $2^3P_0s\bar{s}$ state in the process of Fig. 1a is due to the existence of zero in the wave function $\psi_{M(rad. excit.)}$, see (26). As a result, the convolution of wave functions $\psi_{D_s} \otimes \psi_{M(rad. excit.)}$ occurred to be considerably less than the convolution $\psi_{D_s} \otimes \psi_M$.

So, the production of the radial-excitation state $D_s^+ \rightarrow \pi^+(2^3P_0s\bar{s})$ is relatively suppressed, by the factor of the order of 1/30. This means that by measuring f_0 -resonances one measures actually the yield of the $1^3P_0s\bar{s}$ state.

3.4 The decay $D_s^+ \rightarrow \pi^+ f_0(980)$

The channel $D_s^+ \rightarrow \pi^+ f_0(980)$ dominates the decay $D_s^+ \rightarrow \pi^+ \pi^+ \pi^-$, it comprises $57\% \pm 9\%$. Taking into account the branching ratio $BR(f_0(980) \rightarrow \pi^+ \pi^-) \simeq 53\%$ [11] and the ratio of yields (2), we have:

$$\frac{\Gamma(D_s^+ \rightarrow \pi^+ f_0(980))}{\Gamma(D_s^+ \rightarrow \pi^+ \phi(1020))} = 0.275(1 \pm 0.25) . \quad (28)$$

Calculations performed with formulae (9), (18) and (21) allow one to fulfill this ratio with

$$35^\circ \leq |\varphi| \leq 55^\circ , \quad (29)$$

keeping the charge radius of the D_s^+ -meson in the interval $3.5 \text{ GeV}^{-2} \leq R_{D_s}^2 \leq 5.5 \text{ GeV}^{-2}$, see Fig. 3a.

The data on radiative decays $f_0(980) \rightarrow \gamma\gamma$ and $\phi(1020) \rightarrow \gamma f_0(980)$ tell us that the mixing angle φ can be either $\varphi = -48^\circ \pm 6^\circ$ or $\varphi = 83^\circ \pm 4^\circ$ [9]. The constraint (29) shows that the D_s^+ -meson decay prefers the solution with negative mixing angle, thus supporting the $f_0(980)$ to be dominantly flavour-octet state. The analysis of hadronic spectra in terms of the K-matrix approach [11, 12] also points to the flavour-octet origin of the $f_0(980)$.

3.5 The decay $D_s^+ \rightarrow \pi^+ f_2(1270)$

Taking into account $BR[f_2(1270) \rightarrow \pi^+\pi^-] \simeq 57\%$, one has

$$\frac{\pi^+ f_2(1270)}{\pi^+ \phi(1020)} = 0.09(1 \pm 0.2) . \quad (30)$$

The values of φ_T , which satisfy the ratio (30), are shown in Fig. 3b. With $R_{D_s}^2 \simeq 3.5 \div 5.5 \text{ GeV}^{-2}$ we have $|\varphi_T| \simeq 20^\circ - 40^\circ$, that does not contradict the data both on hadronic decays and the radiative decay $f_2(1270) \rightarrow \gamma\gamma$ which give $\varphi_T \simeq 0 - 20^\circ$. Therefore, the production of $f_2(1270)$ in $D_s^+ \rightarrow \pi^+\pi^+\pi^-$ agrees reasonably with the weight of $s\bar{s}$ component measured in other reactions.

3.6 Bump near 1430 MeV:

the decays $D_s^+ \rightarrow \pi^0 (f_0(1300) + f_0(1500) + f_0(1200 - 1600))$

In the region 1300–1500 MeV two comparatively narrow resonances $f_0(1300)$, $f_0(1500)$ and the broad state $f_0(1200 - 1600)$ are located (for more detail see [11, 13] and references therein). These resonances are the mixtures of quarkonium states from the multiplets 1^3P_0 and 2^3P_0 and scalar gluonium gg :

$$1^3P_0 s\bar{s}, \quad 1^3P_0 n\bar{n}, \quad 2^3P_0 s\bar{s}, \quad 2^3P_0 n\bar{n}, \quad gg. \quad (31)$$

We denote the probabilities for the f_0 resonance to have $1^3P_0 s\bar{s}$ and $2^3P_0 s\bar{s}$ components as $\sin^2 \varphi[f_0]$ and $\sin^2 \varphi_{rad. excit.}[f_0]$, respectively. Then the amplitude for the production of the S -wave $\pi^+\pi^-$ state due to decays of $f_0(1300)$, $f_0(1500)$ and $f_0(1200 - 1600)$ reads:

$$A(D_s^+ \rightarrow \pi^+(\pi^+\pi^-[\sim 1430\text{MeV}])_S) = \sum_n \frac{m_n \sqrt{\Gamma(D_s^+ \rightarrow \pi^+ f_0(n))} \sqrt{\Gamma_n(f_0 \rightarrow \pi^+\pi^-)}}{m_n^2 - s - im_n \Gamma_n}. \quad (32)$$

Here we are summing over the resonances $n = f_0(1300), f_0(1500), f_0(1200 - 1600)$, with the following parameters [11, 13] (in GeV units):

$$f_0(1300) : \quad m = 1.300, \quad \Gamma/2 = 0.12 ,$$

$$\begin{aligned}
f_0(1500) : \quad & m = 1.500, \quad \Gamma/2 = 0.06, \\
f_0(1200 - 1600) : \quad & m = 1.420, \quad \Gamma/2 = 0.508.
\end{aligned} \tag{33}$$

$\Gamma(D_s^+ \rightarrow \pi^+ f_0(n))$ is determined by Eqs. (9) and (21).

The peak which is seen in the $\pi^+\pi^-$ S -wave near 1430 MeV is determined by both $s\bar{s}$ components in $f_0(1300)$ and $f_0(1500)$ and relative phases of the amplitudes of $f_0(1300)$ and $f_0(1500)$ which govern the interference with the background given by $f_0(1200 - 1400)$. According to the analysis of hadronic decays [11, 13], the mixing angles of these states are in the intervals

$$\begin{aligned}
-25^\circ &\lesssim \varphi[f_0(1300)] &\lesssim 15^\circ, \\
-3^\circ &\lesssim \varphi[f_0(1500)] &\lesssim 18^\circ, \\
28^\circ &\lesssim \varphi[f_0(1200 - 1600)] &\lesssim 38^\circ.
\end{aligned} \tag{34}$$

Different variants of the calculation of the $\pi^+\pi^-$ spectra near 1400 MeV are shown in Fig. 4 for the values of mixing angles in the intervals (34). The following parameters were used in the calculation of the transitions $D_s^+ \rightarrow \pi^+ 1^3P_0 s\bar{s} \rightarrow \pi^+(\pi^+\pi^-)_S$:

$$\begin{aligned}
(1) \quad & \varphi[f_0(1300)] = -7^\circ, \quad \varphi[f_0(1500)] = 7^\circ, \quad \varphi[f_0(1200 - 1600)] = 37^\circ, \\
(2) \quad & \varphi[f_0(1300)] = -25^\circ, \quad \varphi[f_0(1500)] = 17^\circ, \quad \varphi[f_0(1200 - 1600)] = 37^\circ, \\
(3) \quad & \varphi[f_0(1300)] = 17^\circ, \quad \varphi[f_0(1500)] = 17^\circ, \quad \varphi[f_0(1200 - 1600)] = 37^\circ.
\end{aligned} \tag{35}$$

The variants (1) and (2) in Fig. 4a reproduce well the bump observed in the $D_s^+ \rightarrow \pi^+\pi^+\pi^-$ decay: the relative weight of the bump for variants (1), (2) is of the order of $\sim 15\% \div 20\%$ that agrees with measured weight of the peak [1]. The variant (3) demonstrates that with the same signs of mixing angles for $f_0(1300)$ and $f_0(1500)$ the calculated curve gives a dip, not bump, near 1400 MeV.

In Fig. 4 one can also see the results of the calculation performed for the radial excitation state $2^3P_0 s\bar{s}$ (curves (4), (5)). For transitions $D_s^+ \rightarrow \pi^+ 2^3P_0 s\bar{s} \rightarrow \pi^+(\pi^+\pi^-)_S$ the following angles are used:

$$\begin{aligned}
(4) \quad & \varphi_{rad. excit.}[f_0(1300)] = -7^\circ, \quad \varphi_{rad. excit.}[f_0(1500)] = 7^\circ, \\
& \varphi_{rad. excit.}[f_0(1200 - 1600)] = 37^\circ, \\
(5) \quad & \varphi_{rad. excit.}[f_0(1300)] = -25^\circ, \quad \varphi_{rad. excit.}[f_0(1500)] = 17^\circ, \\
& \varphi_{rad. excit.}[f_0(1200 - 1600)] = 37^\circ.
\end{aligned} \tag{36}$$

These curves illustrate well the suppression rate of the production of the $2^3P_0 s\bar{s}$ in the decay $D_s^+ \rightarrow \pi^+\pi^+\pi^-$.

The decay $D_s^+ \rightarrow \pi^+\pi^+\pi^-$ was discussed in [3, 4, 5] from the point of view of determination of the quark structure of the resonances produced — let us stress the differences in the obtained results. In the paper [5] the hypothesis of the four-quark structure of $f_0(980)$ is advocated: to explain a large yield of $f_0(980)$ within the four-quark model one needs to assume that the decay $D_s^+ \rightarrow \pi^+\pi^+\pi^-$ goes with a strong

violation of the $1/N_c$ expansion rules. Recall that in terms of the $1/N_c$ expansion the processes shown in Fig. 1a,c,d dominate; it is not clear why these rules, though working well in other decay processes, are violated in $D_s^+ \rightarrow \pi^+\pi^+\pi^-$. From the point of view of Ref. [5], the yield of $s\bar{s}$ state is seen only at larger masses, such as the 1400-MeV bump or higher.

In papers [3, 4] the spectator mechanism shown in Fig. 1a is considered as a dominant one: the authors conclude that $s\bar{s}$ component dominates the resonance $f_0(980)$ — here our conclusions are similar. However, the interpretation of the bump around 1430 MeV differs from ours. Our calculations show that the production of $2^3P_0s\bar{s}$ component is suppressed, so the bump at 1430 is a manifestation of the $1^3P_0s\bar{s}$ component, while it was stated in [3, 4] that the component $2^3P_0s\bar{s}$ is responsible for this bump.

Let us emphasize again that, according to our calculations, relative suppression of the production of $2^3P_0s\bar{s}$ component is due to the use of realistic wave functions of radial-excitation states, see (26): the existence of a zero in the wave function results in a suppression of the convolution $\psi_{D_s} \otimes \psi_{2^3P_0s\bar{s}}$.

4 Conclusion

The performed calculations allow one to trace out the destiny of the $s\bar{s}$ component in the dominating process $D_s^+ \rightarrow \pi^+ + s\bar{s} \rightarrow \pi^+ + f_0$ of Fig. 1a. We show that this transition is realized mainly due to the $1^3P_0s\bar{s}$ state while the production of radial-excitation state, $2^3P_0s\bar{s}$, is suppressed by factor 1/30 or more. Therefore, the reaction $D_s^+ \rightarrow \pi^+ + f_0$ is a measure of the $1^3P_0s\bar{s}$ component in the f_0 mesons.

The data of Ref. [1] tell us that $1^3P_0s\bar{s}$ is dispersed as follows: about 2/3 of this state is hold by the $f_0(980)$ and the last 1/3 is shared between the states with masses in the region 1300–1500 MeV which are $f_0(1300)$, $f_0(1500)$ and broad state $f_0(1200 - 1600)$. This result is quite recognizable as concern the percentage of the f_0 -states produced in the decay $D_s^+ \rightarrow \pi^+\pi^+\pi^-$: $BR(\pi^+f_0(980)) = 57\% \pm 9\%$ and $BR(\pi^+f_0(\text{bump at } 1430 \text{ MeV})) = 26\% \pm 11\%$. The performed calculations demonstrate that nothing prevents this straightforward interpretation. In other words,

- (i) the spectator mechanism $D_s^+ \rightarrow \pi^+ + s\bar{s} \rightarrow \pi^+ + f_0$ dominates,
- (ii) the production of the 2^3P_0 states is suppressed, and
- (iii) the interference of the states $f_0(1300)$, $f_0(1500)$, $f_0(1200 - 1600)$ may organize a bump with the mass ~ 1400 MeV and width ~ 200 MeV.

The data [1] cannot provide us with more scrupulous information about the weight of $1^3P_0s\bar{s}$ component in the resonances $f_0(1300)$, $f_0(1500)$ and $f_0(1750)$ and the broad state $f_0(1400 - 1600)$. To get such information, one needs to carry out a combined analysis of the decay $D_s^+ \rightarrow \pi^+\pi^+\pi^-$ and hadron reactions with the production of investigated resonances. The performed investigation of the reaction

$D_s^+ \rightarrow \pi^+ \pi^+ \pi^-$ is quite in line with the K -matrix analysis of hadronic reactions [11, 12, 13] that tells us that in scalar–isoscalar sector the lowest $1^3P_0 q\bar{q}$ state is the flavour octet while the flavour singlet is a heavier one.

The authors thank A.V. Anisovich and A.V. Sarantsev for useful discussions. The paper is supported by RFFI grant N 01-02-17861.

References

- [1] E791 Collaboration, E.M. Aitala, et al. Phys. Rev. Lett. **86**, 765 (2001).
- [2] E. Klempt, in *Hadron Spectroscopy: Ninth International Conference*, ed. by D.Amelin and A.M.Zaitsev, Melville, NY, 2002, p. 463-482.
- [3] F. Kleefeld, E. van Beveren, G. Rupp, and M.D. Scadron, Phys. Rev. D **66**:034007 (2002).
- [4] P. Minkowski and W. Ochs, hep-ph/0209223 (2002).
- [5] H.Y. Cheng, hep-ph/0212117 (2002).
- [6] D.I. Melikhov, Phys. Rev. D **56**, 7089 (1997);
D.I. Melikhov and B. Stech, Phys. Rev. D **62**:014006 (2000).
- [7] FOCUS Collaboration, J.M. Link et al. Phys. Lett. B **541**, 227 (2002).
- [8] V.V. Anisovich, D.I. Melikhov, and V.A. Nikonov, Phys. Rev. D **52**, 5295 (1995); Phys. Rev. D **55**, 2918 (1997).
- [9] A.V. Anisovich, V.V. Anisovich, and V.A. Nikonov, Eur. Phys. J. A **12**, 103 (2001);
A.V. Anisovich, V.V. Anisovich, V.N. Markov, and V.A. Nikonov, Yad. Fiz. **65**, 497 (2002) [Phys.Atom.Nucl. **65**, 497, (2002)].
- [10] A.V. Anisovich, V.V. Anisovich, V.N. Markov, M.A. Matveev, and A.V. Sarantsev, J. Phys. G: Nucl. Part. Phys. **28**, 15 (2002).
- [11] V.V. Anisovich and A.V. Sarantsev, hep-ph/0204328 (2002), Eur. Phys. J. A (2003), in press;
V.V. Anisovich, V.A. Nikonov, and A.V. Sarantsev, Yad. Fiz. **65**, 1583 (2002) [Phys. Atom. Nucl. **65**, 1545 (2002)].
- [12] V.V. Anisovich and A.V. Sarantsev, Phys. Lett. B **382**, 429 (1996);
V.V. Anisovich, Yu.D. Prokoshkin, and A.V. Sarantsev, Phys. Lett. B **389**, 388 (1996).
- [13] V.V. Anisovich, hep-ph/0208123 (2002).

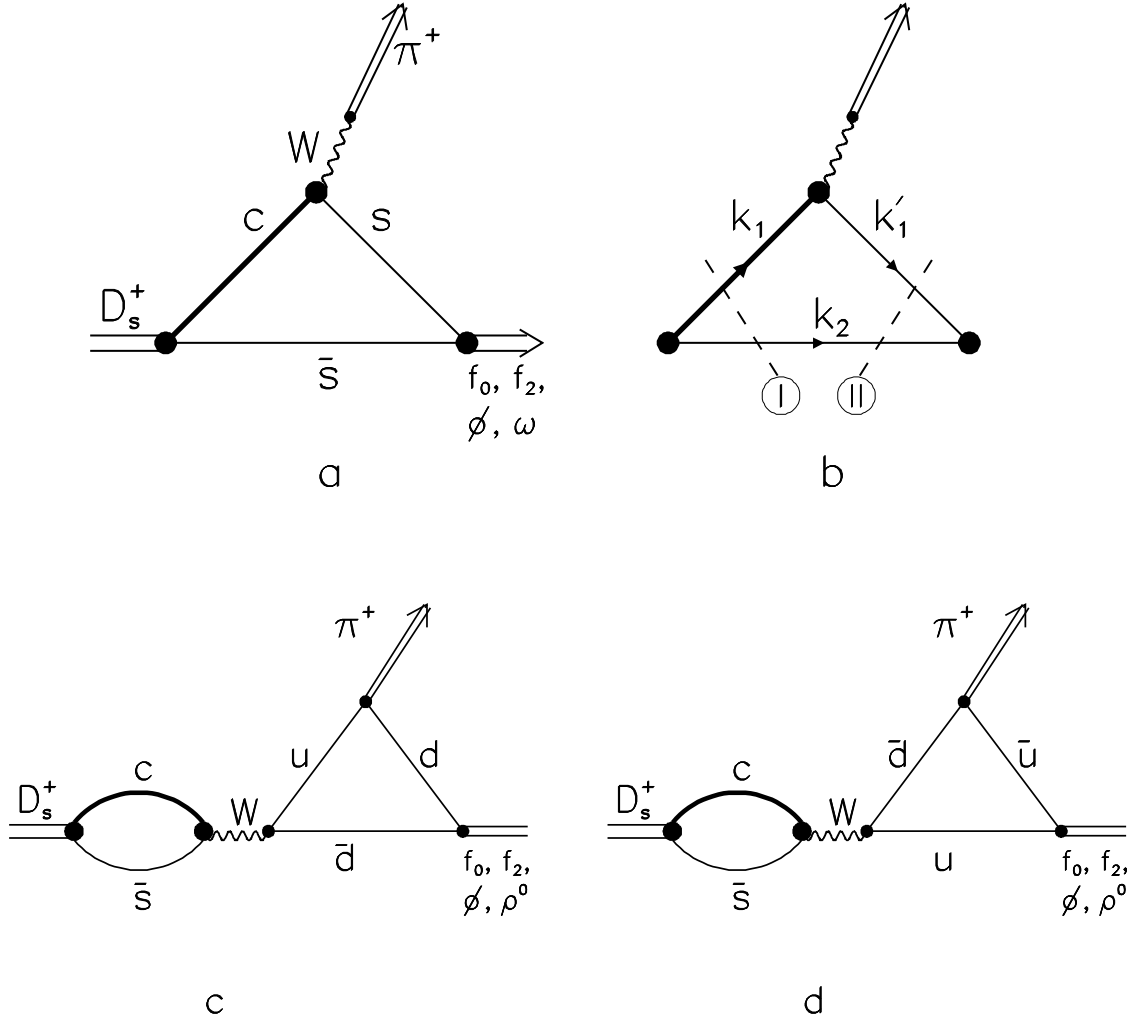


Figure 1: Diagrams determining the decay $D_s^+ \rightarrow \pi^+ \pi^+ \pi^-$: a) diagram for the spectator mechanism; b) energy-off-shell triangle diagram for the integrand of the double spectral representation; c,d) diagrams for the W -annihilation mechanism $D_s \rightarrow u\bar{d}$, with subsequent production of $u\bar{u}$ and $d\bar{d}$ pairs.

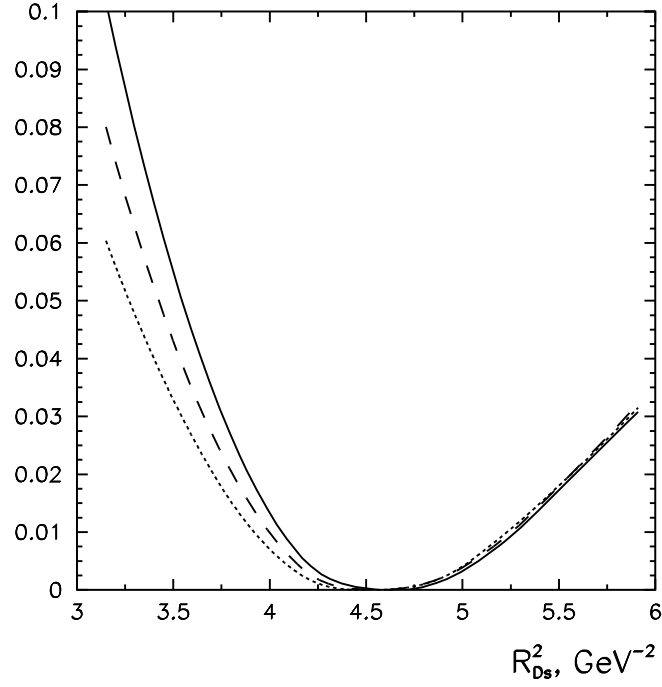


Figure 2: The ratio $\Gamma(D_s^+ \rightarrow \pi^+ f_0^{rad. excit.}) / \Gamma(D_s^+ \rightarrow \pi^+ f_0^{basic})$ as a function of radius square of the D_s^+ meson, see Eq. (13). Calculations have been carried out at fixed $R^2[f_0^{basic}] = 10 \text{ GeV}^{-2}$ for several values of $R^2(f_0^{rad. excit.})$: 10 GeV^{-2} (solid line), 13 GeV^{-2} (dashed line) and 16 GeV^{-2} (dotted line).

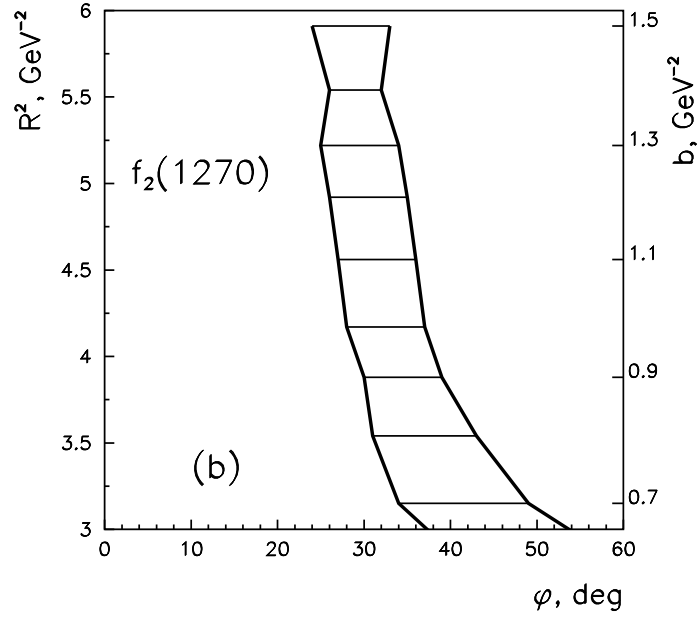
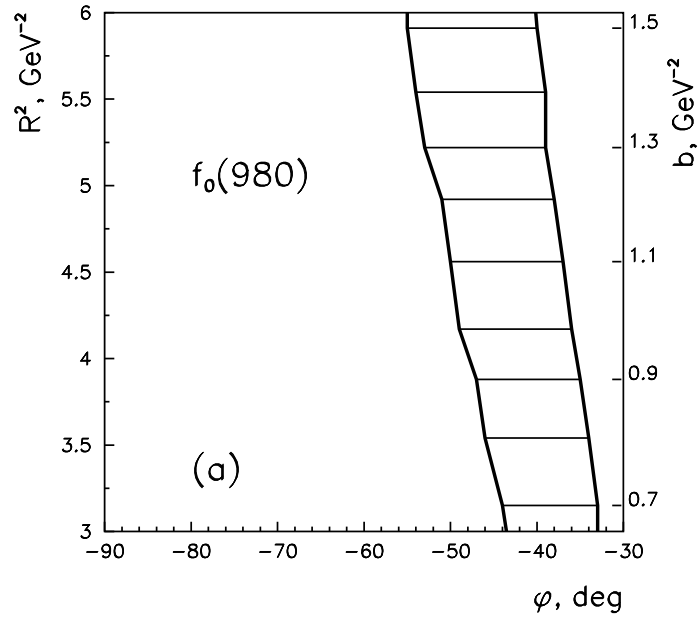


Figure 3: Allowed areas $(R_{D_s}^2, \varphi_M)$ for flavour wave functions (22) provided by experimental constraints (28) and (30).

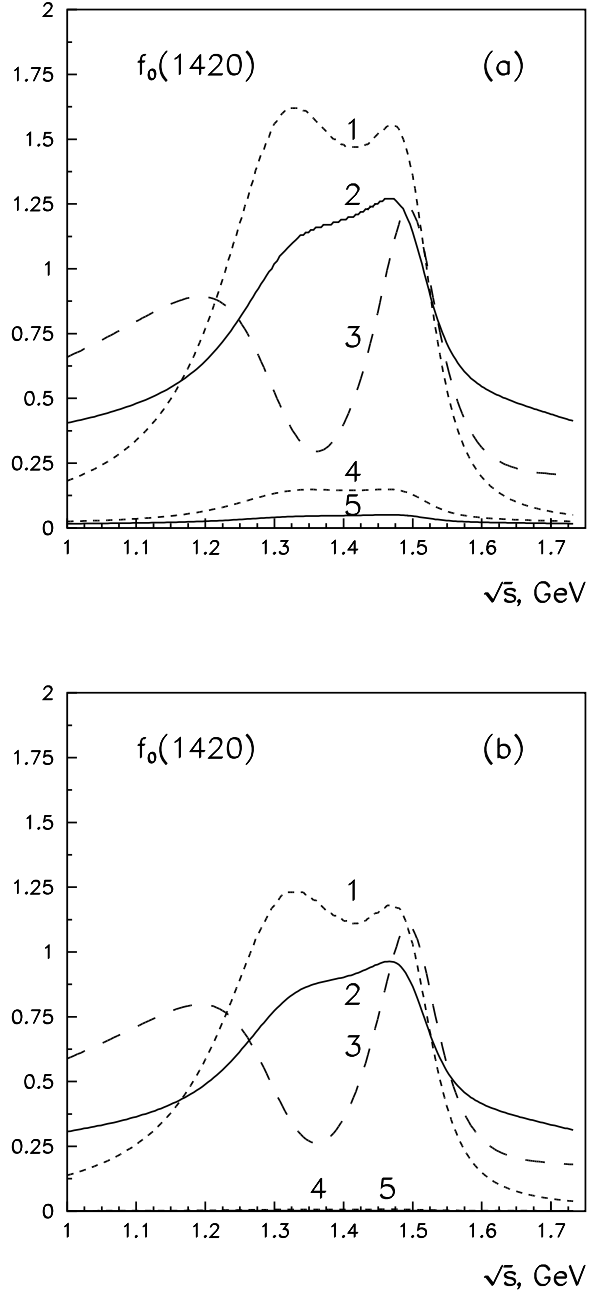


Figure 4: The $\pi^+\pi^-$ mass spectrum in the vicinity of 1430 MeV: calculated curves respond to the production of $f_0(1300)+f_0(1500)$ and the broad state $f_0(1200-1600)$, with $R_{D_s}^2 = 4.15 \text{ GeV}^{-2}$ (a) and $R_{D_s}^2 = 5.90 \text{ GeV}^{-2}$ (b). Parameters used in calculations are given in (35) and (36).